UCLA
COMPUTATIONAL AND APPLIED MATHEMATICS

High Resolution Schemes for Conservation Laws in Simulation of Injection Systems

U. Iben
E. Tadmor

February 2000

CAM Report 00-06

Department of Mathematics
University of California, Los Angeles
Los Angeles, CA. 90095-1555

http://www.math.ucla.edu/applied/cam/index.html

High resolution schemes for conservation laws in simulation of injection systems

U. Iben* and E. Tadmor†

February 11, 2000

Abstract

We present numerical results for different finite difference schemes of first and second order applied to special cases of Euler equations. In these numerical simulations we used a model of a shock tube (piston problem) and a simplified injection system of the Diesel engine or gasoline engine. Several cases that include friction in the pipe are considered.

1 Introduction and mathematical background

In the last five years, a rapid technical development of the Diesel and gasoline injection systems and anti block systems had been started. The resulting systems have a complex technical structure consisting of several complicated subsystems [2]. A simplified model of a gasoline injection system consists of a reservoir, a connected pipeline, and a valve. The mathematical modeling of these systems leads to conservation laws with special initial and boundary conditions. The interpretation of the conservation laws as an evolution equation for cell averages in the finite volume discretization appears to be particularly well suited and physically motivated. The continuity, the momentum, and the energy equations with special source terms (that we call fundamental equations) describe the state of flow in such a model of injection system. The fundamental equations are mathematical relations among the pressure p, the velocity v, the specific internal energy e, the friction forces F, the density ρ and the heating flux q.

The numerical simulation of the injection system is very important for technical interpretations. For injection systems as well as for anti block systems, the aim is to prevent cavitation and strong shocks. Cavitation as well as shocks damage the pipes or valves. Reasonably fast methods with high accuracy are needed for the numerical simulation. For injection systems, numerical simulations with high accuracy help to optimize the injection process in order to save fuel, to optimize the combustion process and to replace unreasonable and costly experiments.

Usually finite difference schemes are used for the simulation in commercial tools. Finite difference schemes of first order, e.g. Lax-Friedrich scheme (LxF), include high damping effects for a large number of time steps. First order Godunov type schemes are considerably more difficult to implement since they require the solution of Riemann problems, and due to the CFL-condition (Courant-Friedrich-Levy), a large number of time steps is necessary to maintain high accuracy. Damping effects are also included. To achieve higher resolution, higher order schemes are needed. Three-point finite difference schemes of second order on fixed uniform grids lead to oscillations. Recently, five-point nonoscillatory finite difference schemes were developed by E. Tadmor et.al. starting with [17, 12]. The main idea behind the construction of these central finite difference schemes is to use more precise information of the local propagation speed. Beyond these CFL related speeds, no characteristics information is required and in particular, the costly (approximate)

*Institut für Analysis und Numerik, Otto-von-Guericke-Universität Magdeburg, PSF 4120 D-39106 Magdeburg; current address: Robert Bosch GmbH, Dept. FV/FLP, P.O.Box 106050, D-70049 Stuttgart, Germnay. Email: uwe.iben@de.bosch.com

†Department of Mathematics, UCLA, Los Angeles, CA 90095. Email: tadmor@math.ucla.edu

Riemann solvers are avoided. In this case the conservative formulation is used. The scheme can be implemented in a straightforward manner as black-box solvers for different applications. The other approach to the second order finite difference schemes considered in this paper is described in [9] for the special case of Euler equations. It can be applied to weak shocks, and after switching to the first order locally, also for strong shocks. Since the scheme is strongly oriented towards the physical behavior of the model, the pressure-velocity-temperature (p-v-T) formulation is used. The velocity v and the pressure p vary on the 1- and 2-characteristics C^+ and C^-. In contrast, the temperature varies on the path of a particle. Injection systems include several mathematical challenges: On one hand, the functional relation between the pressure, density and temperature is not algebraic. On the other hand, shocks and low Mach-numbers can appear in a subdomain of the computational box.
The paper is organized as follow: In this section, the complete system of equations are presented. Section 2 deals with the numerical methods. In Section 3 the simulation of two models - the piston problem and the injection problem - are presented. The final discussion appraises the numerical results and gives an overview for further research problems.

Let us consider unsteady flow of compressible liquid in a finite interval $\omega \subset \mathbb{R}$ and a time interval $(0,T)$ with $0 < T < \infty$. The integral form of the conservation laws for a pipeline with a weak variable cross-sectional area $A = A(z,t)$ reads:

$$\begin{aligned} \int_\omega \frac{\partial}{\partial t}(\rho A)\mathrm{d}z + \int_\omega \frac{\partial}{\partial z}(\rho v A)\mathrm{d}z &= 0, \\ \int_\omega \frac{\partial}{\partial t}(\rho v A)\mathrm{d}z + \int_\omega \frac{\partial}{\partial z}\left(\rho v^2 A + pA\right)\mathrm{d}z - \int_\omega p\frac{\partial A}{\partial z}\mathrm{d}z, &= \int_\omega \rho A F \mathrm{d}z \\ \int_\omega \frac{\partial}{\partial t}\left[\rho A\left(e+\frac{v^2}{2}\right)\right]\mathrm{d}z + \int_\omega \frac{\partial}{\partial z}\left[\rho v A\left(e+\frac{p}{\rho}+\frac{v^2}{2}\right)\right]\mathrm{d}z + \int_\omega p\frac{\partial A}{\partial t}\mathrm{d}z &= \int_\omega q\pi d\mathrm{d}z. \end{aligned} \tag{1.1}$$

The function v denotes the velocity of the fluid, p is the pressure, ρ is the density, F describes the friction forces[1], and q is the heating flux per area with the dimension $[N/(ms)]$. We assume that the cross-sectional area A is a circle. The friction force is defined as a function of the shear stress on the wall λ_{in}, the diameter d of the pipe and the velocity v, i.e.

$$F = -\frac{\lambda_{in}}{2d} v \mid v \mid . \tag{1.2}$$

The value λ_{in} is a function of the Reynolds-number, Re, so that the laminar as well as turbulent flow is modeled, [4]. In addition to the system (1.1), the thermo-dynamical and calorical equation of state is given. Since $A = A(z,t)$, the conservative system (1.1) admits additional low order as source terms on right hand side. In this case we write (1.1) as

$$\int_\omega \left(\frac{\partial}{\partial t}\mathbf{u} + \frac{\partial}{\partial z} f(\mathbf{u})\right)\mathrm{d}z = \int_\omega g(\mathbf{u})\mathrm{d}z, \tag{1.3}$$

where $\mathbf{u}$ is the three dimensional vector of conservative variables and is given by

$$\mathbf{u} = (A\rho, A\rho v, A\rho(e + v^2/2))^\top.$$

The flux function f is

$$f(\mathbf{u}) = \begin{pmatrix} \rho v A \\ \rho v^2 A + pA \\ \rho v A\left(e + \frac{p}{\rho} + \frac{v^2}{2}\right) \end{pmatrix}$$

and the right hand side becomes

$$g(\mathbf{u}) = \begin{pmatrix} 0 \\ \rho A F + p\frac{\partial A}{\partial z} \\ q\pi d - p\frac{\partial A}{\partial t} \end{pmatrix}.$$

[1] friction forces on the wall of the pipe

The system (1.1) is the general integral representation. It is augmented with several boundary and initial conditions depending on which technical application is considered. In general, the boundary conditions are ordinary differential equations. For simplicity we consider elementary boundary conditions with prescribed boundary values.
A simplification of (1.1) is a (2×2) so-called p-system, where the dissipation does not lead to a significant increase in entropy. We shall consider this system in Section 2.1.
In order to prevent rounding errors, the differential equations are purposely scaled. Therefore we fix a reference length L_0, a reference diameter D_0 for the other geometrical values, e.g. the cross-sectional area, a reference pressure p_0, a reference density ρ_0, and a reference sound speed c_0.

2 Numerical methods

In this section we present the basic ideas of the different numerical methods used below. One of the goals is to implement high-resolution schemes that work very fast and are easy to implement in complex simulation tools. The challenge of the numerical simulation is: *Using coarse simply structured grids to achieve high resolution in a short computational time.*
In our calculations below we used a characteristic method, three different types of first order finite difference schemes, and two finite difference schemes of second order. The four first-order schemes include the well-known Courant-Isaacson-Rees (CIR), Lax-Friedrichs (LxF) and its localize version (lLxF) and a first order characteristics based schemes. We turn now to second order schemes.
The first scheme *AFVM* (adaptive finite volume scheme) is based on a three-point stencil. To get a second order scheme, the domain of dependence is adapted to the state of flow. As mentioned above, three-point difference schemes of second order on fixed grids lead to oscillations. Since for a weak compressive liquid the density ρ and the value ρv vary only on a small interval, the scheme AFVM is based on the p-v-T formulation of the equation (1.1). In contrast, the pressure p varies on a significantly larger scale. The scheme is stable and does not need the CFL-condition to satisfy the stability condition. Therefore it is very flexible for simulations. We do not restrict time-stepping. A detailed introduction to the scheme AFVM is given in [9]. We use uniform mesh in space $\{z_j\}$ and time $\{t_n\}$. The discrete values of space and time dependent functions for instance, the discrete values of pressure p, are denoted by $p(z_j, t_n) = p_j^n$. The time step is denoted by Δt, the space step by Δz. The explicit *AFVM* scheme for (1.1) is a two-step scheme of the form:

$$
\begin{aligned}
p_j^{n+1} &= p_M - \frac{c_M^2 \Delta\tau}{2(z_R - z_L) A_M b_M c_0} (\rho_R v_R A_R - \rho_L v_L A_L) \\
v_j^{n+1} &= v_M + \frac{v_M \Delta\tau}{2(z_R - z_L)\rho_M A_M c_0} (\rho_R v_R A_R - \rho_L v_L A_L) \\
&\quad - \frac{\Delta\tau}{2(z_R - z_L)\rho_M A_M c_0} (\rho_R v_R^2 A_R - \rho_L v_L^2 A_L) \\
&\quad - \frac{\Delta\tau}{2(z_R - z_L)\rho_M A_M c_0} (p_R A_R - p_L A_L) \\
&\quad + \frac{\Delta\tau}{2(z_R - z_L)\rho_M A_M c_0} (A_R - A_L) p_M + \frac{\Delta\tau}{2c_0} F_M \\
T_j^{n+1} &= T_M + \frac{\alpha_M T_M}{\rho_M c_{pM}} (p - p_M) + \frac{\Delta\tau}{2 c_{pM} c_0} (q_u - v_M F_M)
\end{aligned}
\tag{2.1}
$$

with $q_u = (q\pi d)/(\rho A)$ denoting the heat flow per mass union. The values with the indices L and R indicate the values along the respective left and right characteristics. The values with the index M are defined by the path, see Figure 0.1. The term $\Delta\tau$ is the time step defined by $\Delta\tau = \Delta t \cdot c_0$, where c_0 is a fixed reference sound of velocity mentioned above.

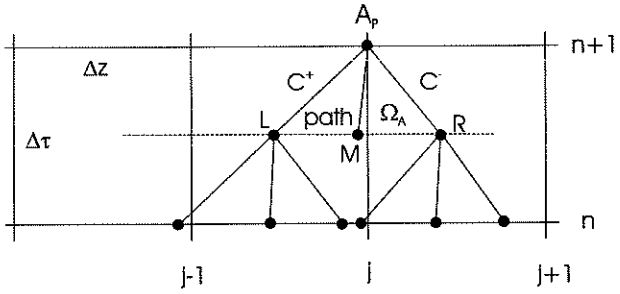

Figure 0.1: Computational procedure for AFVM

We now turn to the other second order scheme introduced by Kurganov and Tadmor [12] which is based on the conservative formulation given in (1.3). We will use the semi-discrete formulation which is very flexible and can be used in explicit or implicit forms. The CFL-condition with the CFL-number $\lambda_{CFL} = \Delta\tau/\Delta z < 1/\lambda_{\max}$ is necessary to guarantee the stability of the scheme. To write the scheme in a compact form, several notations are introduced. The term $\mathbf{u}_j^n$ denotes the discrete values of the vector of the conservative values on mesh introduced above. To evolve in time, we introduce the midvalues:

$$\mathbf{u}_{j+1/2}^{+} = \mathbf{u}_{j+1}^n - \frac{\triangle z}{2} D\mathbf{u}_{j+1}^n, \quad \mathbf{u}_{j+1/2}^{-} = \mathbf{u}_j^n + \frac{\triangle z}{2} D\mathbf{u}_j^n. \tag{2.2}$$

Here, the midvalues $\mathbf{u}^{\pm}$ are obtained as endpoints of piecewise linear reconstruction based on the nonoscillatory numerical derivatives $D\mathbf{u}$. The numerical derivative of the function $\mathbf{u}$ is computed component-wise. Here is a library of such nonoscillatory numerical derivatives, [12]. For a numerical approximation of the numerical derivatives on the grid point (x_j, t_n) we use

$$D\mathbf{u}_j^n = MinMod\left(\frac{\mathbf{u}_{j+1}^n - \mathbf{u}_j^n}{\triangle z}, \frac{\mathbf{u}_j^n - \mathbf{u}_{j-1}^n}{\triangle z}\right).$$

In order to ensure that the scheme is non-oscillatory, we use the $MinMod$ function, given by

$$MinMod(x,y) = \frac{1}{2}\left(sgn(x) + sign(y)\right)\min\{|\ x\ |, |\ y\ |\}, \quad x, y \in \mathbb{R}.$$

If x and y are vectors, then the $MinMod$ function has to be implemented for each component. This choice of numerical derivative may over smear a strong discontinuity, where the order of accuracy is less significant. Other possible choices for $D\mathbf{u}_j^n$ are given in [10, 17]. We denote the Jacobian of the flux function f by $D_f F$. The values $\lambda_{i,j}^n$ are the eigenvalues of three dimensional matrix $D_J f(\mathbf{u}_j^n)$. The maximal eigenvalue in each cell is given by

$$a_{j+1/2}^n = \max_{s=j,j+1} \max_{i=1,2,3} \{|\ \lambda_{i,s}^n\ |\}.$$

The Kurganov Tadmor scheme (KT) takes the form

$$\begin{aligned} \frac{\partial \mathbf{u}_j}{\partial t} =& -\frac{1}{2\triangle z}\left(f(\mathbf{u}_{j+1/2}^{+}) + f(\mathbf{u}_{j+1/2}^{-}) - f(\mathbf{u}_{j-1/2}^{+}) - f(\mathbf{u}_{j-1/2}^{-})\right) \\ &+ \frac{1}{2\triangle z}\left(a_{j+1/2}^n(\mathbf{u}_{j+1/2}^{+} - \mathbf{u}_{j+1/2}^{-}) - a_{j-1/2}^n(\mathbf{u}_{j-1/2}^{+} - \mathbf{u}_{j-1/2}^{-})\right) + g(\mathbf{u}_j^n) \\ &:= F_f(\mathbf{u}^n)_j + g(\mathbf{u}_j^n). \end{aligned} \tag{2.3}$$

Here $\mathbf{u}^n$ denotes the vector of discrete points on the time level n. The right hand side of (2.3) is a second order approximation of $f(\mathbf{u})_z + g(\mathbf{u})$. If we use a forward finite difference to approximate the time derivative, we get an explicit first order Euler scheme. For higher order dicretizations in

time we may use for instance Runge-Kutta-methods or related methods. In this case, we will use the Heun scheme which is given by the predictor and corrector step

$$\begin{aligned} \mathbf{u}_j^* &= \mathbf{u}_j^n + \Delta t \left[F_f(\mathbf{u}_j^n) + g(\mathbf{u}_j^n)\right], \\ \mathbf{u}_j^{n+1} &= \mathbf{u}_j^n + \frac{\Delta t}{2}\left(\left(F_f(\mathbf{u}^n)_j + g(\mathbf{u}_j^n)\right) + \left(F_f(\mathbf{u}^*)_j + g(\mathbf{u}_j^*)\right)\right), \end{aligned} \tag{2.4}$$

for details see [11, 15]. The present approach is considerably simpler than second order upwind Godunov type methods, which requires the complete knowledge of a single Riemann solution and special transformations between the representation in Euler and Lagrange coordinates, [1]. If the source term is stiff, then the scheme can be formulated as an implicit one for which several methods of solution are derived. Using Crank-Nicholson scheme for (2.3), we have

$$\begin{aligned} \mathbf{u}_j^{n+1/2} &= \mathbf{u}_j^n + \frac{\Delta t}{2}\left[F_f(\mathbf{u}_j^n) + g(\mathbf{u}_j^n)\right], \\ \mathbf{u}_j^{n+1} - \frac{\Delta t}{2} g(\mathbf{u}_j^{n+1}) &= \mathbf{u}_j^n + \Delta t F_f(\mathbf{u}^{n+1/2})_j + \frac{\Delta t}{2} g(\mathbf{u}_j^n). \end{aligned} \tag{2.5}$$

The *KT* scheme (2.3) is a five-point difference scheme. Due to the influence of the boundary values on the numerical solution it is necessary to approximate the conditions very accurately. The boundary conditions consist of a strong reflection on the right and an outflow boundary condition on the left side of the computational box. For staggered grids, non-oscillatory boundary treatments were developed in [14]. Similar formulas exist for non-staggered grids. There are different approaches to handle the boundary conditions including three-point stable schemes which are used on the boundary. In this case one has to guarantee that the scheme is stable. The boundary conditions propagate along the characteristics to retain high accuracy of the interior scheme.

To compare the different numerical properties of first and second order schemes the numerical tests are done with six different schemes. We use a typical upwind scheme by Courant-Isaacson-Rees *CIR* [19, p.362], the adaptive finite volume scheme given in (2.1), the well-known first order Lax-Friedrichs scheme

$$\mathbf{u}_j^{n+1} = \frac{\mathbf{u}_{j+1}^n + \mathbf{u}_{j-1}^n}{2} - \frac{\lambda_{CFL}}{2}\left(f(\mathbf{u}_{j+1}^n) - f(\mathbf{u}_{j-1}^n)\right), \ \lambda_{CFL} = \frac{\Delta t}{\Delta z},$$

the first order local LxF (lLxF) scheme

$$\begin{aligned} \mathbf{u}_j^{n+1} = \mathbf{u}_j^n &- \frac{\lambda_{CFL}}{2}\left(f(\mathbf{u}_{j+1}^n) - f(\mathbf{u}_{j-1}^n)\right) \\ &+ \frac{\lambda_{CFL}}{2}\left(a_{j+1/2}^n(\mathbf{u}_{j+1}^n - \mathbf{u}_j^n) - a_{j-1/2}^n(\mathbf{u}_j^n - \mathbf{u}_{j-1}^n)\right), \end{aligned}$$

and the KT scheme given in (2.4). Finally, a second order method of characteristics (*SCM*), [3], is implemented for further comparison of numerical results. A general review on upwind schemes, high resolution and limiters is given in [18].

2.1 The KT scheme applied to a liquid and gas flow

We assume that the cross-sectional area A of the pipe is constant. The p-system with the friction force on the wall and the time $\tau = c_0 t$ is

$$\frac{\partial}{\partial t}\begin{pmatrix} \rho \\ \rho v \end{pmatrix} + \frac{\partial}{\partial z}\begin{pmatrix} \rho v \\ \rho v^2 + p \end{pmatrix} = \begin{pmatrix} 0 \\ \rho F \end{pmatrix}. \tag{2.6}$$

We apply equation (2.6) to an initial boundary value problem of a liquid flow and gas flow. The increase in entropy due to the friction force is neglected.

A straightforward computation gives the eigenvalues of the Jacobian $D_J f$:

$$\lambda_1 = \frac{v-c}{c_0} \quad \text{and} \quad \lambda_2 = \frac{v+c}{c_0}.$$

Applying (2.3) for each component we get:

$$\begin{aligned}
c_0 \frac{\partial \rho_j^n}{\partial \tau} &= -\frac{1}{2\triangle z}\left((\rho v)^+_{j+1/2} + (\rho v)^-_{j+1/2} - (\rho v)^+_{j-1/2} - (\rho v)^-_{j-1/2}\right) \\
&\quad + \frac{1}{2\triangle z}\left(a_{j+1/2}\left(\rho^+_{j+1/2} - \rho^-_{j+1/2}\right) - a_{j-1/2}\left(\rho^+_{j-1/2} - \rho^-_{j-1/2}\right)\right), \\
c_0 \frac{\partial (\rho v)_j^n}{\partial \tau} &= -\frac{1}{2\triangle z}\left((\rho v^2 + p)^+_{j+1/2} + (\rho v^2 + p)^-_{j+1/2} - (\rho v^2 + p)^+_{j-1/2} - (\rho v^2 + p)^-_{j-1/2}\right) \\
&\quad + \frac{1}{2\triangle z}\left(a_{j+1/2}\left((\rho v)^+_{j+1/2} - (\rho v)^-_{j+1/2}\right) - a_{j-1/2}\left((\rho v)^+_{j-1/2} - (\rho v)^-_{j-1/2}\right)\right) \\
&\quad + (\rho F)_j^n.
\end{aligned} \tag{2.7}$$

Further we have

$$a_{j+1/2} = \max\left\{|\,(v-c)_j\,|, |\,(v+c)_j\,|, |\,(v-c)_{j+1}\,|, |\,(v+c)_{j+1}\,|\right\}.$$

The discretization in space is of second order. Explicit discretization in time of second order, e.g. the Heun scheme or Runge-Kutta scheme, lead to a complete second order discretization.
We briefly discuss the initial and boundary problem for a weak compressive fuel. The KT scheme computes the density ρ and the velocity v on a fixed grid. The pressure p has to compute by $\rho = \rho(p;T)$ using the inverse function or an iteration process. For a liquid, the functional relation between the speed of sound c, the pressure p and the density is measured by experiments, [8]. In contrary to the KT scheme, the AFVM is based on the primitive variables p and v, which are computed in each computational step, consult Section 3.2.
The gas flow is considered without friction. In addition to the p-system with zero right side, the equation of isentropic state

$$p(\rho) = p_0\left(\frac{\rho}{\rho_0}\right)^\kappa$$

is used, where $\kappa = c_p/c_v$. The value c_p is the specific heat at constant pressure and c_v at constant volume respectively. The values p_0 and ρ_0 are fixed values.

3 Numerical results

In this section numerical results for different numerical methods on two important technical models are presented. All methods are implemented in *FORTRAN90* code. The figures are done in *MATLAB* code.

3.1 A pipe with a periodic working piston

We consider a pipe of length $L = 10$ m with a periodic working piston on the left side. For short, it is called the *piston problem*. The pipe is filled with an ideal gas (air). We are interested in the values of pressure on the right side which is denoted with $K3$. From the technical point of view it is very important to compute the pressure p dependent on $K3$. The left boundary is denoted by $K1$. Figure 0.2 contains the model of the pipe with the piston and the computational domain.

The boundary condition on K1 is the velocity

$$v_k = v_{\max} \sin\left(\frac{2\pi\tau}{T_s c_0}\right), \quad \tau \geq 0$$

which is the model of the oscillating piston. The value T_s is the period of oscillation and $v_{\max}$ is the maximum of the speed. For the numerical example we chose different $v_{\max}$ and T_s. The sound of velocity for air is $c_0 = 330$ m/s. The acceleration at $\tau = 0$ has the maximum $b_m(\tau = 0) = 2\pi v_{\max}/T_s$. It depends on the boundary and initial conditions whether shocks appear or not. In the case of a shock, the beginning of the shock τ_s can be computed analytically, i.e.

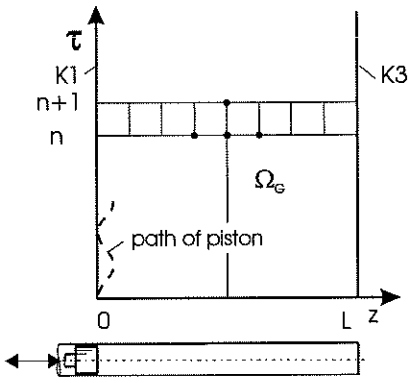

Figure 0.2: Piston problem

$$\tau_s = \frac{2}{\kappa + 1} \frac{c_0^2}{b_p(0)}.$$

The following numerical schemes are implemented:

- first order Lax-Friedrich scheme (LxF)
- local first order Lax-Friedrich scheme (lLxF)
- second order characteristic method (SCM)
- first order Courant-Isaacson-Rees scheme(CIR)
- second order adaptive finite volume scheme (AFVM)
- second order Kurganov-Tadmor scheme (KT)

There are several methods to compute the solution from the time level t^n to t^{n+1}. On one hand, we use a fixed CFL-number λ_{CFL}. On the other hand, the CFL-number is chosen as large as it is possible for each time step in order to save time steps. The first strategy is used for the LxF, the lLxF and the KT schemes. The second strategy is used for the CIR scheme where a large number of time steps is saved.
The CFL-condition is satisfied for the SCM automatically. Using the c, v-formulation, we get the compatibility conditions of the SCM

$$\begin{aligned} c + \frac{\kappa - 1}{2} v &= const \quad \text{on } C^+\text{-characteristic}, \\ c - \frac{\kappa - 1}{2} v &= const \quad \text{on } C^-\text{-characteristic} \end{aligned}$$

For this reason, the c, v-formulation implemented in the method of characteristics is used when comparing the numerical results with the results by LxF, lLxF and KT schemes for the piston problem.
Let us denote the number of points in space as $\#N$ and in time as $\#T$.

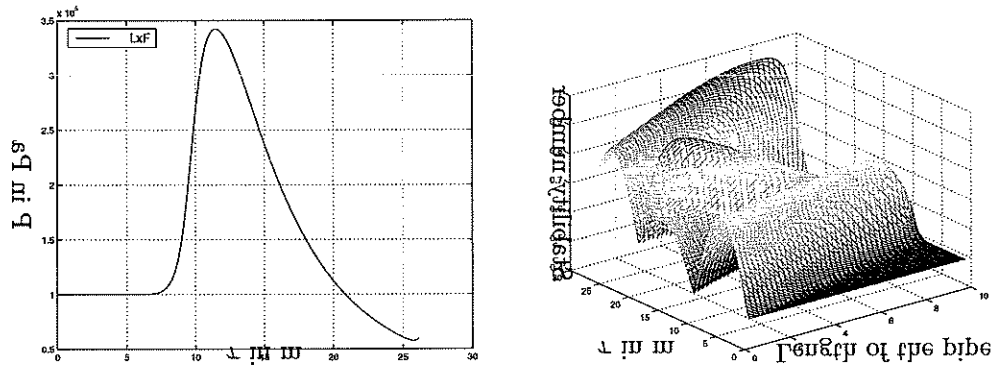

Figure 3.1: LxF scheme with $\Delta z/\Delta t = 2$: Pressure on $K3$ and stability number

method	$v_{\max}$	T_S	Δz	$\Delta\tau$	CFL-number	$\#N$	$\#T$	order
-	m/s	s	m	m	-	-	-	
CIR	15	5.53e-2	2.5e-2	2.120e-2	optimal	80	440	first
SCM	15	5.53e-2	2.5e-2	2.500e-2	-	80	200	second
LxF	15	5.53e-2	2.5e-2	6.250e-3	0.5	80	961	first
lLxF	15	5.53e-2	2.5e-2	1.325e-3	0.5	80	961	first
KT	15	5.53e-2	2.5e-2	1.325e-3	0.85	80	570	second
CIR	15	2.78e-2	1.25e-3	1.223e-3	optimal	80	440	first
SCM	15	2.78e-2	1.25e-3	1.250e-3	-	80	200	second
LxF	15	2.78e-2	1.25e-3	3.125e-4	0.5	80	961	first
lLxF	15	2.78e-2	1.25e-3	1.250e-4	0.5	80	961	first
KT	15	2.78e-2	1.25e-3	1.250e-4	0.6	80	800	second
CIR	50	5.53e-2	7.5e-4	7.251e-4	optimal	80	653	first
SCM	50	5.53e-2	7.5e-4	7.500e-4	-	80		second
LxF	50	5.53e-2	7.5e-4	1.875e-4	0.5	80	961	first
lLxf	50	5.53e-2	7.5e-4	7.500e-5	0.5	80	961	first
KT	50	5.53e-2	7.5e-4	1.125e-4	0.6	80	800	second
CIR	172	5.53e-2	3.75e-5	3.610e-5	optimal	320	3400	first
SCM	172	5.53e-2	3.75e-5	3.750e-5	-	320	1600	second
LxF	172	5.53e-2	3.75e-5	1.875e-5	0.25	320	7680	first
lLxf	172	5.53e-2	3.75e-5	1.875e-5		320	-	first
KT	172	2.78e-2	3.75e-5	1.875e-5	0.15	320	13530	second

Table 1: Numerical results for the piston problem

The first, second and third cases in Table 1 are typical situations for technical tools in pneumatic systems.
The last case of the Table 1 corresponds to the *resonance* case. In this situation, the main difficulty is to handle the shocks due to the increase of the shock strength. As a result of this behavior the CFL-number has to be chosen very small in order to guarantee the stability of the schemes. Figure 1 contains the CFL-number as a function of the time τ and the space. For further time steps the stability number (which has to be < 1 in each computational time step)

$$\Delta\tau/\Delta z * \lambda_{\max} = \frac{\Delta\tau}{\Delta z}\left(\frac{|\,v\,|+c}{c_0}\right)$$

becomes greater than one, so that the stability is not guaranteed any more.
There is a main difference between the finite difference schemes and the method of characteristics. The finite difference schemes do not compute the exact position of reflections on the boundary K3 and shocks in the pipe on a coarse grid. The speed of propagation is too fast. The perturbation

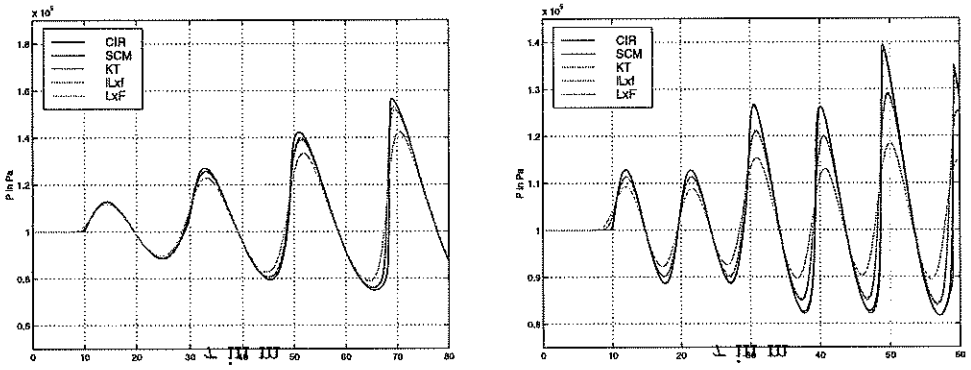

Figure 3.2: Pressure on $K3$: $\#N = 80$ for $T_s = 5.53e-2$ s and $T_s = 2.76e-2$ s, $v_{\max} = 15$m/s

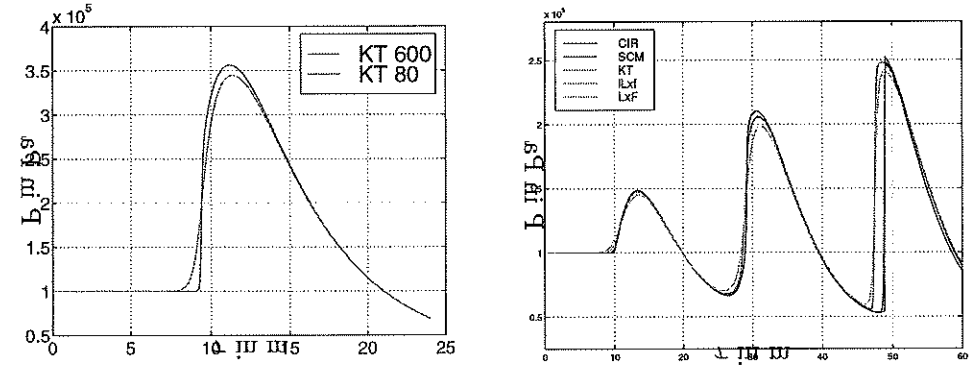

Figure 3.3: Pressure on $K3$: $\#N = 80$, $\#N = 600$ and $\#N = 80$ for $T_s = 5.53e-2$ s, $v_{\max} = 172$ s

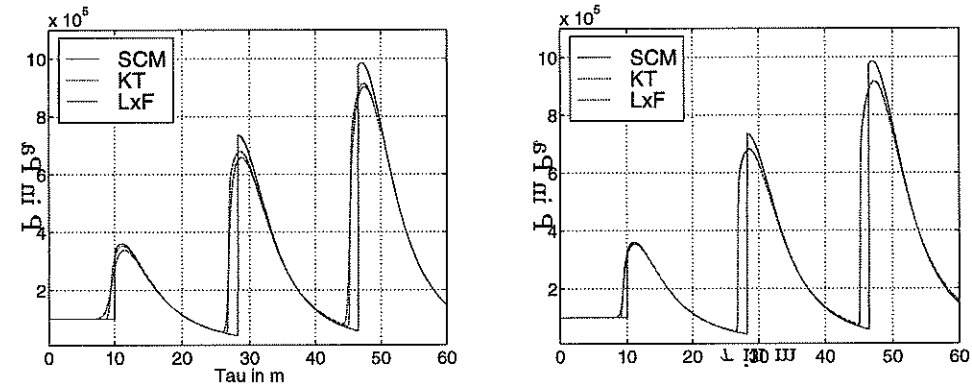

Figure 3.4: Pressure on $K3$: $\#N = 160$ and $\#N = 320$ for $v_{\max} = 172$ m/s and $T_s = 5.53e-2$ s - case of *natural resonant frequency*

provoked by the piston reaching the boundary $K3$ in a time $\tau \approx 10$ m. The SCM identifies this time point accurately. If we increase the number of grid points in z-direction, the KT scheme localizes the reflection on the boundary K3 at $\tau = 9.65$ m which is a more precise time than $\tau = 8.2$ m in the case of $\#N = 80$, see Figure 3. On the other side, finite difference schemes are very flexible schemes which are easy to implement.

3.2 The Common Rail Diesel injection system

The simplified Common Rail Diesel injection system consists of a reservoir with a constant pressure, a pipe of the length $L = 1.5\,\mathrm{m}$ and a controlled valve, see Figure 0.3 where the model and the computational domain is given. The valve on the right side called K3 is controlled. The pressure in the combustion chamber following the valve is fixed by $p_{cc} = 78$ bar.

The valve opens at $t = 0$ and the opening cross-sectional area increases linearly up to $t_o = 2\,\mathrm{ms}$. It starts closing with $t_{sc} = 7.66\,\mathrm{ms}$ and is completely closed at $t_c = 9.33\,\mathrm{ms}$. All geometrical data of our model are taken from an injection system of a medium-speed large Diesel engine. The time difference $t_c - t_{sc}$ influences the maximal pressure occurred in the process. The pressure in the reservoir varies from $p_{res} = 550$ bar to 750 bar for the numerical simulations. We assume that the pressure is constant during the simulation process. Using conservative variables, the pressure p has to compute by the functional expressions $\rho = \rho(p;T)$ and $c = c(p;T)$ with the inverse function or in the case that it is not an analytical expression by an iteration process (bisection or Newton procedure). The iteration procedure has to be chosen very carefully due to the derivative ρ_p is very small for large values p in the case of a fuel. For our numerical simulation, the following ansatz is used:

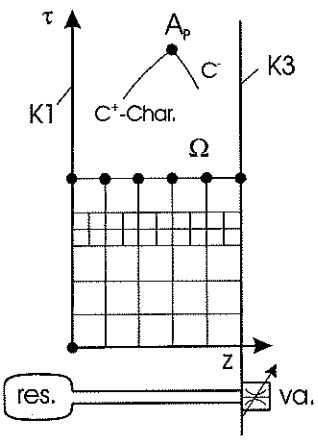

Figure 0.3: Common Rail system

$$\rho = a_1 + a_2 p + a_3 T + a_4 p^2 + a_5 T p + a_6 T^2 + a_7 p^3 + a_8 p^2 T + a_9 p T^2 + a_{10} T^3,$$

where T is a fixed temperature and a_i are real values depending on the fuel. They are determined by experiments. The p-system is implemented where additional properties are considered in the programming code:

1. a cavitation model,
2. the friction forces on the wall, see (1.2)
3. the elasticity module of the pipe,
4. the leakages by vortex as a result of contraction of the flow at the inlet (reservoir - pipe) are considered by a one-dimensional model, see [7] for details,
5. rate of detached air in the liquid, the ratio - mass of air and mass of liquid - is given by 10^{-8}.

The chosen cavitation model is a simple thermodynamical model found in the literature, see [6]. In contrast to many other codes, e.g. *AMESim* [13] we compute the steam production on the basis of the thermodynamical equilibrium. In the case of cavitation the value $p_{steam} = 0.08$ bar

for $T = 304$ K have been taken for water, see [16, p. 449], due to the respective value for fuel is not given in the literature.
Due to the boundary conditions and the properties of the liquid a *low Mach-number problem* is available; when we recall $Ma = \frac{v}{c}$ with $c^2 = \frac{dp(\rho;T)}{d\rho}$ for fuel. Low Mach-number problems are treated in [5]. We do not want to discuss that problem in detail. Using the conservative variables can lead to ill-conditioned problems and due to this fact, formulations in primitive variables are preferred. In Figure 6, the stability number for $\Delta\tau = \Delta z$ and the Mach-number Ma are plotted. Thus, the finite difference schemes LxF and KT need a CFL-number $\lambda_{CFL} \leq 0.6$ to guarantee numerical stability.
Let us denote the number of points in space as $\#N$ and in time as $\#T$. The computational time is denoted by ct.

method	p_{res}	t_{sc}	Δz	$\Delta\tau$	CFL-number	$\#N$	$\#T$	ct
-	bar	ms	m	m	-	-	-	hour
AFVM	550	7.66	5.90e-3	5.90e-3	-	150	4050	0.8
KT	550	7.66	5.90e-3	2.95e-3	0.5	150	8000	1.8
LxF	650	6.66	5.90e-3	2.95e-3	0.5	150	8000	1.8
SCM	650	6.66	5.90e-2	4.69e-3	-	150	4050	0.7
AFVM	650	6.66	5.90e-2	4.69e-3	-	150	4050	0.8
KT	650	6.66	5.90e-3	2.95e-3	0.5	150	8000	2.3
LxF	650	7.66	5.90e-3	2.95e-3	0.5	150	8000	1.8
SCM	650	7.66	5.90e-2	4.69e-3	-	150	4050	0.7
AFVM	650	7.66	5.90e-2	4.69e-3	-	150	4050	0.8
KT	650	7.66	5.90e-3	2.95e-3	0.5	150	8000	2.3
LxF	750	7.66	5.90e-3	2.95e-3	0.5	150	8000	1.8
SCM	750	7.66	5.90e-2	4.69e-3	-	150	4050	0.7
AFVM	750	7.66	5.90e-2	4.69e-3	-	150	4050	0.8
KT	750	7.66	5.90e-3	2.95e-3	0.5	150	8000	2.3

Table 2: Numerical results for the Common Rail system

The difference of the numerical results computed by SCM and AFVM differs by 1.2%. Due to this fact, we define the solution computed with AFVM as the exact solution in order to compare the numerical solutions computed with LxF and KT schemes.
We compare the numerical solutions. The first example with $p_{res} = 550$ bar includes cavitation due to the computed pressure p becoming smaller than the stream pressure $p_{steam} = 0.08$ bar for $T = 304$ K see Figure 7. The differences in the numerical solutions are the maxima of pressure, the wave period being smaller and the influence of the cavitation process being greater for the KT scheme than for the AFVM.
Figure 5 contains the results for $p_{res} = 650$ bar and $0 \leq \tau \leq 40$ m for SCM and AFVM; for the LxF scheme and the KT scheme. Two essential differences appear in the results. First, the maxima of the pressure p computed with LxF and KT schemes are greater than those for the AFVM or SCM respectively. The difference amounts approximately 12%. Second, the velocity of the phase is greater for the LxF and KT schemes in contrast to the AFVM. Further, in Figure 7 we compare the numerical results for $p_{res} = 750$ bar up to a time $0 \leq \tau \leq 50$ m for the LxF, KT scheme and AFVM. In this case, similar differences in the numerical results between the schemes appear.
Several difficulties appear in the numerical simulation of the injection systems using conservative variables:

1. The computation of the pressure p in (2.6) by $\rho = \rho(p;T)$ using an iteration process. Therefore the functional relation between ρ and p for fixed temperature T has to be known, for details see Figure 9. In the case of a variable temperature (increased by a shock) the functional relation is a two-dimensional surface.

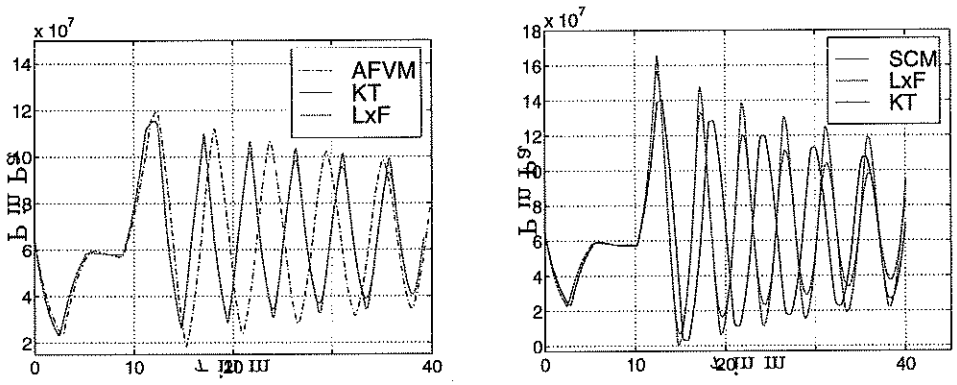

Figure 3.5: Pressure on K3: $p_{res} = 650$ bar, $p_{cc} = 78$ bar, $t_{sc} = 6.566$ ms and $t_{sc} = 7.66$ ms $\#N = 150$

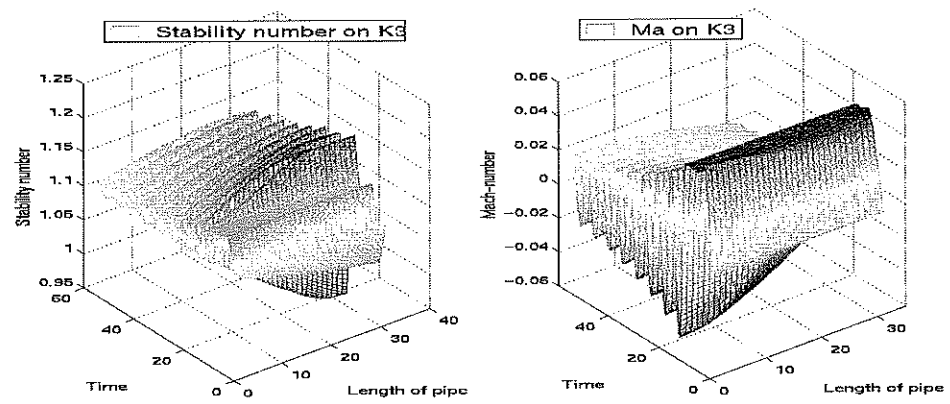

Figure 3.6: Stability number and Mach-number for $p_{res} = 850$ bar, $p_{cc} = 78$ bar and $t_{sc} = 7.66$ ms

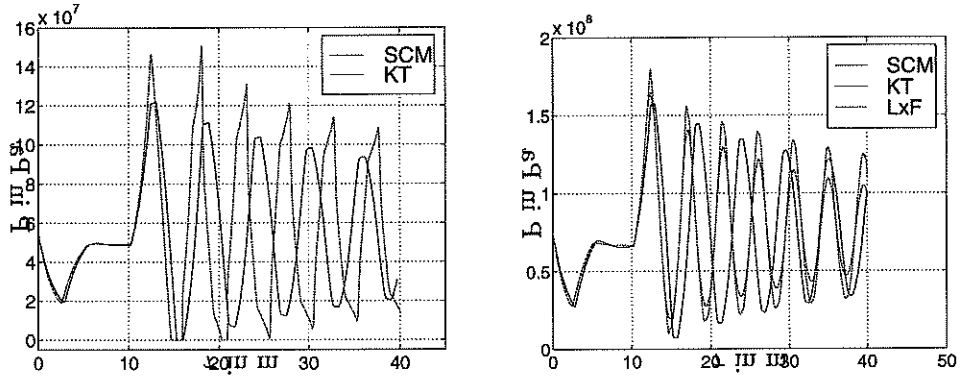

Figure 3.7: Pressure on K3: $p_{res} = 550$ bar and $p_{res} = 750$ bar, $p_{cc} = 78$ bar, $t_{sc} = 7.66$ ms, $\#N = 150$

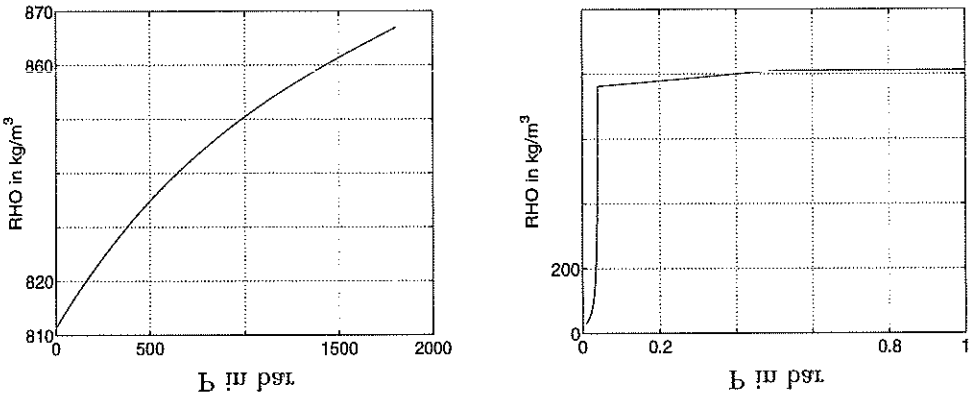

Figure 3.8: Functional relation between the pressure p and the density ρ for $T = 303$ K

2. The cavitation model based on information of the steam pressure p_{steam} is difficult to implement due to the computation of the pressure p by an iteration process which requires additional computational time. Further, all experimental data are given as a discrete function $p = p(\rho; T)$.

3.3 Final discussion and further research problems

It is obvious that the finite difference schemes, except the LxF scheme, lead to the same numerical results for small amplitudes of pressure and large wave periods, compare Figure 2. In the case of higher pressure maxima and smaller wave periods larger differences in the numerical solutions appear.
In contrast to the first order schemes, the KT scheme resolves the shocks with a higher accuracy. On the other hand, due to the CFL-number, the numerical computations require a larger number of time steps than for SCM or AFVM. For the piston problem, the central difference schemes as well as the characteristic method and the AFVM lead to nearly the same results. One difference is the computational speed which is lower in the case of the central schemes. The largest benefit of the central schemes (especially the second order schemes) are the resolution of shocks and the easy implementation.
The injection model contains the low Mach-number problem which is difficult to handle. The formulation and simulation using the primitive variables is more effective than the formulation in conservative variables and leads to a fast simulation procedure for this problem. Due to the computation of the pressure by an iteration process the computational time increases.
For the simulation of technical applications three issues are decisive

1. the flexibility of the numerical algorithm,
2. the accuracy of the numerical results for large and small computational scales,
3. and the computational speed.

All tested algorithms do not optimize the three demands. The finite difference schemes CIR, lLxF, LxF, KT are very flexible but for a high accuracy the computational speed is low. The SCM and AFVM have a high accuracy but the algorithms are not very flexible in contrast to the other schemes. The challenge is the construction of numerical algorithms which combine the properties mentioned above.
The simulation of injection systems with a complete cavitation model, e.g. with the implementation of the *Henry law*, is a further challenge. Additional to the modeling problem of cavitation, the low Mach-number problems appears. The sound speed drops from $c = 1200$ m/s to 40 m/s in a very small subdomain of the computational area. In this case, local refinement of the computational mesh in an a posteriori process is necessary.

Acknowledgments. The work has been supported in part by the DFG-Priority Research Project *Analysis and Numerics for Conservation Laws*, Wa 633-10, NSF Grant No. DMS97-06827 and ONR Grant No. N00014-1-1076.

References

[1] M. Ben-Artzi and J. Falcovitz, *Second-order godunov-type scheme for compressible fluid dynamics*, Journal of Computayional Physics, 55 (1984), pp. 225–255.

[2] E. Brucker, *Die Entwicklung des Common-Rail-Einspritzsystems für die Baureihe 4000*, MTZ, Sonderausgabe (1997).

[3] C.Hirsch, *Numerical computation of internal and external flows*, John Wiley and Son, 1988.

[4] R. Fox and A. McDonald, *Introduction to Fluid Mechanics*, John Willey and Sons, Inc., 1994.

[5] H. Guillard and C. Viozat, *On the behaviour of upwind schemes in low Mach number limit*, Computers and Fluids, 28 (1997), pp. 63–86.

[6] I. Harbke and H.-K. Iben, *Modelling and calculation of the cavitation in transient pipeline flows*, MTZ, 1 (1998), pp. 60–64.

[7] H.-K. Iben and U. Iben, *Ein beitrag zur modellierung der kavitation und der ranbedingungen eines stark kompressiblen fluides in instationaeren leitungsströmungen*, preprint nr. 03, Uni Magdeburg, Fakultät für Maschinenbau, 1999.

[8] H.-K. Iben and I. Kosmowski, *Ein Beitrag zum Druck-, Dichte-, Temperaturverhalten von Dieselkraftstoff und Schwerölen*, Wiss. Zeitschrift, TH Magdeburg, 1979.

[9] U. Iben and H.-K. Iben, *A modified finite volume scheme and the simulation of wave movement on a simplified diesel injection system*, System analysis and modelling simulation, ** (1999), p. ****.

[10] G. Jiang, D. Levy, C. Lin, S. Osher, and E. Tadmor, *High-resolution nonoscillatory central schemes with nonstaggered grids for hyperbolic conservation laws*, SIAM J. Numer. Anal., 35 (1998), pp. 2147–2168.

[11] D. Jordan and P. Schmith, *Nonlinear ordinary differential equations*, Claredon Press Oxford, 1977.

[12] A. Kurganov and E. Tadmor, *New high-resolution central schemes for nonlinear conservation laws and convection-diffusion equations*, tech. rep., UCLA CAM Report, 99-16, 1999.

[13] S. Lausanne, ed., *Numerical Challenges Posed by Modelling Hydraulic Systems*, Forum on Design Languages, 1998.

[14] D. Levy and E. Tadmor, *Non-oscillatory boundary treatment for staggered central schemes*, submitted, (1999).

[15] W. Luther, K. Niederdrenk, F. Reutter, and H. Yserentant, *Gewöhnliche Differentialgleichungen*, Vieweg-Verlag, 1987.

[16] S. Mayinger, *Thermodynamik*, Springer-Verlag, 1992.

[17] H. Nessyahu and E. Tadmor, *Non-oscillatory central differencing for hyperbolic conservation laws*, Journal of Computational Physics, 87 (1990), pp. 408–463.

[18] E. TADMOR, *Approximate solutions of nonlinear conservation laws*, in Advanced Numerical Approximation of Nonlinear Hyperbolic Equations (A. Quateromi, ed.) Lecture Notes in Mathematics no. 1697, Springer, (1998), pp. 1–150.

[19] W. TÖRNIG AND P. SPELLUCCI, *Numerische Mathematik für Ingenieure und Physiker*, vol. 2, Springer-Verlag, 1990.